Controlling deformation in a high quality factor silica microsphere toward single directional emission

Jin-Ming Cui,[1] Chun-Hua Dong,[1] Chang-Ling Zou,[1] Fang-Wen Sun,[1,*]
Yun-Feng Xiao,[2] Zheng-Fu Han,[1] and Guang-Can Guo[1]

[1]Key Lab of Quantum Information, University of Science and Technology of China, Hefei 230026, Anhui, China

[2]State Key Lab for Mesoscopic Physics, School of Physics, Peking University, Beijing 100871, China

*Corresponding author: fwsun@ustc.edu.cn

Received 12 October 2012; revised 25 November 2012; accepted 2 December 2012;
posted 10 December 2012 (Doc. ID 177963); published 10 January 2013

High-Q deformed silica microsphere cavities are fabricated by short CO_2 laser pulses, where the deformation is well controlled by adjusting the intensity and number of pulses. Using this method, directional emission from whispering-gallery mode (WGM) with a high quality factor of 10^7 in these microspheres is achieved, and a transition from two-directional to single-directional emission is observed. Such concentrated directional emission and high-Q of WGMs show high potential for future studies of the chaotic ray dynamics in deformed microcavity and cavity quantum electrodynamics and optomechanics.

OCIS codes: 140.3410, 230.5750, 350.3950.

Whispering-gallery mode (WGM) microresonators with smoothly deformed boundaries named as asymmetric resonant cavities have been hotly discussed to test classical and quantum chaos recently [1,2]. These deformed microresonators can support directional emission modes, which provide an easy way to excite and detect cavity mode via free space. Various shapes of asymmetric resonant cavities, such as quadrupole [3–5], microstadium [6–8], egg-shaped [9], limacon-shaped [10,11], Gibbous-shaped [12], and spiral-shaped microcavity [13,14] have been intensively investigated both theoretically and experimentally in the past few years. The microresonators, combined with highly directional emission and ultrahigh quality factor, have been thought to be promising candidates for ultralow threshold microlasing and controllable single photon source. However, there is a tradeoff between the directionality and quality factor. On the one hand, microcavities, such as those with a spiral-shaped and limacon-shaped boundaries support unidirectional emission modes, but their quality factors are typically below 10^5. On the other hand, experiments have realized directional emissions with high Q WGMs [15]; however, they didn't achieve single directional emission. Also, they lack a practical method to control the deformation and directional emission of these asymmetric cavities.

In this paper, we used a controllable way to to deform silica microspheres with various emission directions and high-Q (about 10^7) modes. CO_2 laser pulse modification method [15] was further researched and a controllable way was developed by experimentally analyzing the sphere boundary variation under different pulse conditions. The deformation can be well controlled by adjusting the intensity and interaction number of heating laser pulses. Along with increasing the deformation, a transition of two-directional to single-directional emission was observed, indicating the underlying dynamical tunneling mechanism of directional emission. Combined with theoretical simulation [12], this work provides a way to design, control, and fabricate single directional microspheres, which have the potential application to support further research, such as studies of chaotic ray dynamics in a deformed

1559-128X/13/020298-04$15.00/0

microcavity, strong-coupling cavity quantum electrodynamics [16], high sensitive sensors [17], and quantum optomechanics [18].

Silica microspheres with various diameters ranging from 20 to 100 μm can be fabricated by CO_2 laser beam. Due to the scattering losses on residual surface inhomogeneities and surroundings, the Q factors of these microspheres are between 10^7 and 10^8 [19]. Top view images of these spheres are captured by a high resolution CCD through a microscope [Fig. 1(b)], and their boundaries are extracted by image processing technology. During the microsphere fabrication process, the whole sphere is heated by a continuous CO_2 laser to a steady thermal state, which is almost isotropic. The sphere surface tension makes the boundary of equator plane almost a perfect circle, where the variation is below 0.5% of its radius. The deformation of a microsphere can be induced by shooting CO_2 laser pulses to one side of the microsphere. In this case, the equator of deformation microsphere resembles a Gibbous shape, where its boundary can be approximatively described by a combination of a half-circle and a half-quadrupole [12]:

$$r(\theta) = \begin{cases} R(1 - \epsilon\cos^2\theta) & \text{if } \cos(\theta) \geq 0 \\ R & \text{if } \cos(\theta) < 0 \end{cases}, \qquad (1)$$

where θ represents the polar angle, R is the microsphere radius, and ϵ is taken to describe the deformation. In experiments, the deformation of a microsphere is principally affected by the intensity and width of laser pulses, so the deformation can be controlled by adopting appropriate parameters. To show the effect, microspheres with diameters of approximate 50 μm are chosen to observe the deformation after the reheating laser pulses. As illustrated in Fig. 1(a), the deformation increases by adding more CO_2 laser pulses with a width of 100 ms. There is a threshold of laser power to deform the microsphere. No obvious deformation is observed when the pulse intensity is less than 40 W/mm^2. However, the deformation after one pulse clearly increases with the pulse intensity of 54 W/mm^2. When the intensity is larger than 80 W/mm^2, the microsphere would be destroyed after the short pulse treatment.

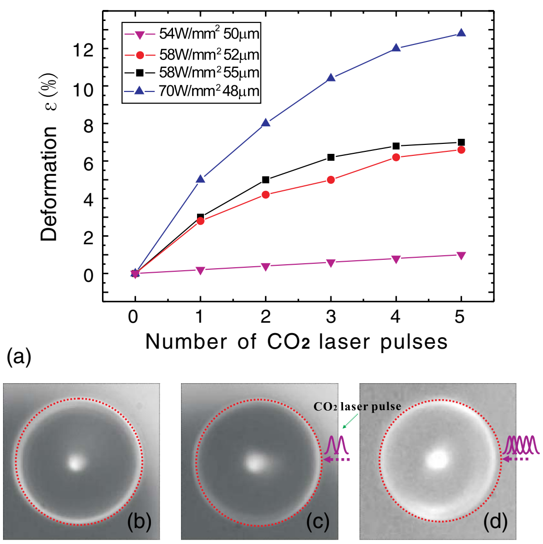

Fig. 1. (Color online) (a) Measured deformation with different CO_2 pulse intensity and number. The legend shows the laser power and microsphere diameter for each line. (b)–(d) Top views of the same microsphere variation with 0, 2, and 5 CO_2 laser pulses from the arrow direction, respectively. The sphere diameter is about 50 μm.

Figures 1(b) and 1(c) show optical images of the boundaries of equator planes before and after applying two short CO_2 laser pulses on one side, respectively, where red dotted curves indicate the ideal circular boundary. With more laser pulses, the degree of deformation can be gradually increased. Figure 1(d) shows a typical optical image of the equator boundary reheated by five CO_2 laser pulses, where the deformation on one side is obvious. It slightly departs from the half-quadrupole because the laser beam can barely reheat the microsphere with perfect axisymmetry.

To investigate the optical characteristics of WGMs in the deformed microspheres, we inject a tunable laser beam at 780 nm (linewidth <300 kHz) band into the fiber taper to excite clockwise WGMs, as shown in Fig. 2(a). The fiber taper with the diameter of about 1 μm is fabricated by the hydrogen microtorch. The transmission is measured by a 125 MHz low-noise photoreceiver. The far-field emission signals from

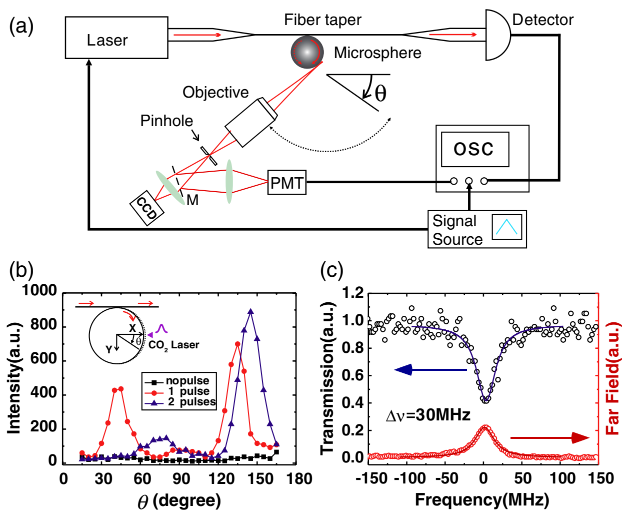

Fig. 2. (Color online) Sketched experimental setup and measurement results. (a) The transmission is directly measured by the photoreceiver and observed through the oscillograph (OSC). The far-field emission signals are detected by the system, composed of a microscope objective (N.A. 0.28), spatial filter with a pinhole, and a PMT. M is a flip mirror. (b) Typical far-field emission patterns from WGMs excited near the x–y plane. θ is the polar angle with respect to the x axis. For squares, circles, and triangles, the in-plane deformation ϵ are estimated to be 0%, 3.0%, and 6.8%, corresponding to no-pulse, 1-pulse, and 2-pulse with pulse power 65 W/mm^2 for same microsphere with the diameter of 50 μm, respectively. Inset: the schematics of the excitation geometry. (c) The transmission (blue) and far field signals (red) are fitted well with Lorentzian-shaped curves with $(\epsilon, \theta) = (6.8\%, 135°)$.

the microsphere boundary are collected by a microscope objective (N.A. 0.28). After the spatial filter with a pinhole, the signals are finally detected by a photomultiplier tube (PMT). The objective, pinhole, and PMT are held on a rotator so that far-field emission can be collected from different directions (corresponding to different θ). In experiments, the presence of tapered fiber near the microsphere will influence the WGMs and its lateral movement will affect measurement results. It is difficult to avoid mechanical perturbation of the substrate and the flow of surrounding air to keep the fiber taper stable during the experiment. Here we contact the fiber taper to the microsphere to make a stable measurement condition.

Figure 2(b) shows far-field emission patterns for a microsphere with diameter of 50 μm, which are obtained by recording the WGM spectra as a function of θ near the equator plane. Without reheating, there is no obvious directional emission from the sphere boundary. After one 65 W/mm^2 pulse reheating with the deformation $\epsilon = 3.0\%$, there are two obvious directions at $\theta = 45°$, 135°. Remarkably, the directional emission at $\theta = 45°$ vanishes when the microsphere is reheated after two pulses with $\epsilon = 6.8\%$, which verifies that the unidirectional emission of WGMs can be observed with the larger deformation ϵ. Figure 2(c) shows the transmission from the fiber taper (the blue curve) and far-field signals from directional emission angle at $\theta = 135°$ (the red curve) with $\epsilon = 6.8\%$. The line width of the mode is about 30 MHz, corresponding to a loaded Q factor of 1.3×10^7.

To understand the evolution of directional emission in the deformed microcavity with increasing deformation, we numerically solve the Maxwell equations by Boundary element method [20]. As shown in Fig. 3(b), the peak around 45° in the far-field distribution reduces with increasing deformation, which is consistent with the observation in our experiments. A typical near-field profile of electric field of clockwise traveling wave WGM is shown in Fig. 3(a) with $2\pi R/\lambda \approx 98.23$ and $\epsilon = 0.10$, where single-direction emission at the boundary is clearly shown. The underlying mechanism of the directional emission can be explained by ray dynamics. As the cavity is deformed slightly, rays are mainly tunneling out tangentially to the cavity boundary. The 5-periodic orbit in the phase space gives rise to two directional emission [21]. When increasing the deformation, the region of chaotic sea increases, and rays tunneling to the chaotic sea. In this case, the emission direction is determined by the short-time ray dynamics, and refracted out from the boundary following the unstable manifolds [2,12]. Since there is no rotational symmetric of the cavity boundary shape, rays tend to be refracted at a selected point on the boundary [as shown in Fig. 3(a)], leading to single directional emission.

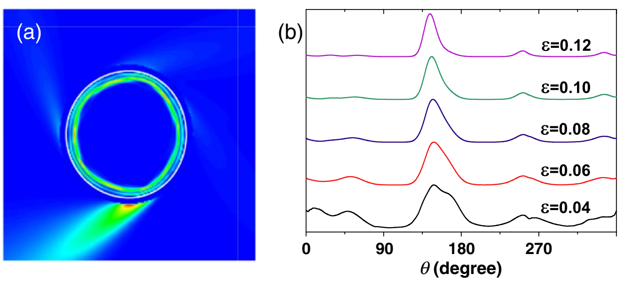

Fig. 3. (Color online) (a) Typical near-field profile of clockwise traveling WGM. The field outside of the cavity is enhanced for visualization. (b) Far-field patterns of WGMs for different deformations by Boundary Element Method simulated wave function.

Actually, the boundary shape of the microsphere cavity can not be precisely measured in experiments, which is slightly different from the half-circle–half-quadrupole shape model studied above. In addition, the rays in the three dimensional microsphere have more degrees of freedom than the two-dimensional model. Therefore, there are some discrepancies between the experimental and theoretical results, especially that the experiment shows highly directional emission at a much smaller deformation. This phenomena has been reported previously in 3D microspheres, where the directional emission can happen with smaller deformation due to the Arnold diffusion in a 3D deformed microcavity [1,4].

In summary, thermal-induced deformed microspheres have been experimentally studied in detail. Highly directional emission and even single directional emission of WGMs are observed by applying two or more short CO_2 laser pulses to reheat the microsphere. The measured loaded Q factors of WGMs in these half-circle–half-quadrupole shaped microspheres can reach 1.3×10^7. These high-Q deformed microspheres are expected to play a significant role in cavity quantum electrodynamics research, especially in strong exciton–photon coupling physics at low temperature.

We acknowledge Y. Yang and X.-W. Wu for fruitful discussions. The work was supported by the 973 Programs (Nos. 2011CB921200 and 2011CBA00200), the National Natural Science Foundation of China (NSFC) (Nos. 11004184 and 11004003), the Knowledge Innovation Project of the Chinese Academy of Sciences (CAS).

References

1. S. Lacey, H. Wang, D. H. Foster, and J. U. Nockel, “Directional tunneling escape from nearly spherical optical resonators,” Phys. Rev. Lett. **91**, 033902 (2003).
2. Y. Xiao, C. Zou, Y. Li, C. Dong, Z. Han, and Q. Gong, “Asymmetric resonant cavities and their applications in optics and photonics: a review,” Front. Optoelectron. Chin. **3**, 109–124 (2010).
3. C. Gmachl, F. Capasso, E. Narimanov, J. Nockel, A. Stone, J. Faist, D. Sivco, and A. Cho, “High-power directional emission from microlasers with chaotic resonators,” Science **280**, 1556 (1998).
4. S. Lacey and H. Wang, “Directional emission from whispering-gallery modes in deformed fused-silica microspheres,” Opt. Lett. **26**, 1943–1945 (2001).
5. J. Yang, S. Moon, S. Lee, J. Lee, K. An, J. Shim, H. Lee, and S. Kim, “Development of a deformation-tunable quadrupolar microcavity,” Rev. Sci. Instrum. **77**, 083103 (2006).
6. T. Harayama, P. Davis, and K. Ikeda, “Stable oscillations of a spatially chaotic wave function in a microstadium laser,” Phys. Rev. Lett. **90**, 063901 (2003).

7. W. Fang, H. Cao, and G. Solomon, "Control of lasing in fully chaotic open microcavities by tailoring the shape factor," Appl. Phys. Lett. **90**, 081108 (2007).
8. S. Mestanza, A. Von Zuben, and N. Frateschi, "Enhanced side-mode suppression in chaotic stadium microcavity lasers," J. Appl. Phys. **105**, 063101 (2009).
9. K. Shima, R. Omori, and A. Suzuki, "High-Q concentrated directional emission from egg-shaped asymmetric resonant cavities," Opt. Lett. **26**, 795–797 (2001).
10. S. Shinohara, M. Hentschel, J. Wiersig, T. Sasaki, and T. Harayama, "Ray-wave correspondence in limacon-shaped semiconductor microcavities," Phys. Rev. A **80**, 031801 (2009).
11. Q. Song, W. Fang, B. Liu, S. Ho, G. Solomon, and H. Cao, "Chaotic microcavity laser with high quality factor and unidirectional output," Phys. Rev. A **80**, 041807 (2009).
12. C. L. Zou, F. W. Sun, C. H. Dong, X. W. Wu, J. M. Cui, Y. Yang, G. C. Guo, and Z. F. Han, "Mechanism of unidirectional emission of ultrahigh q whispering gallery mode in microcavities," arXiv: 0908.3531, IEEE J. Sel. Top. Quantum Electron. (to be published).
13. G. D. Chern, H. E. Tureci, A. D. Stone, R. K. Chang, M. Kneissl, and N. M. Johnson, "Unidirectional lasing from InGaN multiple-quantum-well spiral-shaped micropillars," Appl. Phys. Lett. **83**, 1710–1712 (2003).
14. C. Kim, J. Cho, J. Lee, S. Rim, S. H. Lee, K. R. Oh, and J. H. Kim, "Continuous wave operation of a spiral-shaped microcavity laser," Appl. Phys. Lett. **92**, 131110 (2008).
15. Y. Xiao, C. Dong, Z. Han, G. Guo, and Y. Park, "Directional escape from a high-Q deformed microsphere induced by short CO_2 laser pulses," Opt. Lett. **32**, 644–646 (2007).
16. M. Larsson, K. Dinyari, and H. Wang, "Composite optical microcavity of diamond nanopillar and silica microsphere," Nano Lett. **9**, 1447–1450 (2009).
17. A. M. Armani, R. P. Kulkarni, S. E. Fraser, R. C. Flagan, and K. J. Vahala, "Label-Free, Single-Molecule detection with optical microcavities," Science **317**, 783–787 (2007).
18. V. Fiore, Y. Yang, M. Kuzyk, R. Barbour, L. Tian, and H. Wang, "Storing optical information as a mechanical excitation in a silica optomechanical resonator," Phys. Rev. Lett. **107**, 133601 (2011).
19. C. Dong, C. Zou, J. Cui, Y. Yang, Z. Han, and G. Guo, "Ringing phenomenon in silica microspheres," Chin. Opt. Lett. **7**, 299–301 (2009).
20. C. Zou, H. Schwefel, F. Sun, Z. Han, and G. Guo, "Quick root searching method for resonances of dielectric optical microcavities with the boundary element method," Opt. Express **19**, 15669–15678 (2011).
21. Y. Xiao, C. Dong, C. Zou, Z. Han, L. Yang, and G. Guo, "Low-threshold microlaser in a high-Q asymmetrical microcavity," Opt. Lett. **34**, 509–511 (2009).